J Neurophysiol 98: 527–536, 2007.
First published May 9, 2007; doi:10.1152/jn.00259.2007.

Multichannel Micromanipulator and Chamber System for Recording Multineuronal Activity in Alert, Non-Human Primates

Charles M. Gray, Baldwin Goodell, and Alex Lear
Center for Computational Biology, Department of Cell Biology and Neuroscience, Montana State University, Bozeman, Montana

Submitted 7 March 2007; accepted in final form 5 May 2007

Gray CM, Goodell B, Lear A. Multichannel micromanipulator and chamber system for recording multineuronal activity in alert, non-human primates. *J Neurophysiol* 98: 527–536, 2007. First published May 9, 2007 doi:10.1152/jn.00259.2007. We describe the design and performance of an electromechanical system for conducting multineuron recording experiments in alert non-human primates. The system is based on a simple design, consisting of a microdrive, control electronics, software, and a unique type of recording chamber. The microdrive consists of an aluminum frame, a set of eight linear actuators driven by computer-controlled miniature stepping motors, and two printed circuit boards (PCBs) that provide connectivity to the electrodes and the control electronics. The control circuitry is structured around an Atmel RISC-based microcontroller, which sends commands to as many as eight motor control cards, each capable of controlling eight motors. The microcontroller is programmed in C and uses serial communication to interface with a host computer. The graphical user interface for sending commands is written in C and runs on a conventional personal computer. The recording chamber is low in profile, mounts within a circular craniotomy, and incorporates a removable internal sleeve. A replaceable Sylastic membrane can be stretched across the bottom opening of the sleeve to provide a watertight seal between the cranial cavity and the external environment. This greatly reduces the susceptibility to infection, nearly eliminates the need for routine cleaning, and permits repeated introduction of electrodes into the brain at the same sites while maintaining the watertight seal. The system is reliable, easy to use, and has several advantages over other commercially available systems with similar capabilities.

INTRODUCTION

A widely used technique for monitoring neuronal activity in awake-behaving monkeys is to implant a recording chamber over a craniotomy in the skull and advance electrodes into the brain each day using a microdrive that mounts onto the chamber. The electrodes are typically advanced through the dural membrane or, when deep structures are accessed, they are protected by guide tubes that are advanced into the brain (Asaad et al. 2000; Baker et al. 1999; Cham et al. 2005; Miller et al. 1996; Mountcastle et al. 1991; Prut et al. 1998). This commonly used set of techniques suffers from at least two types of problems: one is related to the type of recording chambers in common usage, and a second is associated with the manipulation of electrodes.

A fundamental difficulty with commonly used recording chambers is that they are not hermetically sealed. This leads to a high incidence of infections within the chamber, thereby risking the health of the animal and increasing the need for daily cleaning. A second problem is that the dural membrane is tough, grows vigorously when exposed, and can dimple substantially when passing multiple microelectrodes. To alleviate this problem, the dura must be repeatedly "thinned" to avoid electrode damage (Spinks et al. 2003) and excessive dimpling. This procedure risks further infection, is time consuming, and is stressful to the animal. Finally, daily implantation of one or more guide tubes through the dura can result in significant damage, potentially cause the animal pain, or further increase the possibility of infection.

The principal problems with currently available micromanipulators are that they are usually limited to one or a few electrodes, and they often employ bulky and/or manual mechanisms for controlling electrode movement, can be difficult to electrically shield, or are quite expensive, putting them beyond the resources of many laboratories (Mountcastle et al. 1991; Reitboeck and Werner 1983). These problems are exacerbated if the experimental questions require monitoring of neuronal activity from more than one region of the brain.

Here we describe the design and performance of a new type of recording chamber and micromanipulator system that can solve or reduce these problems and increase the feasibility for multineuron recording from one or more regions of the brain simultaneously. The chamber system is small, is low in profile, and provides a semi-chronic window onto the brain through the use of a watertight, replaceable Sylastic membrane (Arieli et al. 2002). The membrane is self-sealing, prevents infection and allows multiple electrodes to be easily and repeatedly introduced. The micromanipulator allows the remote control of eight independently moveable microelectrodes, is well shielded and easy to setup and use, and is comparably inexpensive. The control electronics can operate up to eight micromanipulators at a time, making it feasible to monitor neuronal activity from multiple regions of the brain simultaneously.

METHODS

All mechanical design work was performed using SolidWorks, a computer aided design package (SolidWorks). Electrical circuit design and the layout of printed circuit boards were performed using the OrCAD Capture and OrCAD Layout software packages, respectively (Cadence).

Chamber system

The chamber system, shown in Fig. 1, was designed with two objectives in mind. First and foremost, we wanted the intracranial space to be hermetically sealed off from the external environment. This would serve to reduce the chances of infection and help reestablish the normal balance of intracranial pressure. The barrier for maintaining the seal had to permit the passage of microelectrodes without disrupting the seal or damaging the electrodes and ideally

Address for reprint requests and other correspondence: C. M. Gray, Center for Computational Biology, 1 Lewis Hall, Montana State University, Bozeman, MT 59717 (E-mail: cmgray@nervana.montana.edu).

The costs of publication of this article were defrayed in part by the payment of page charges. The article must therefore be hereby marked "*advertisement*" in accordance with 18 U.S.C. Section 1734 solely to indicate this fact.

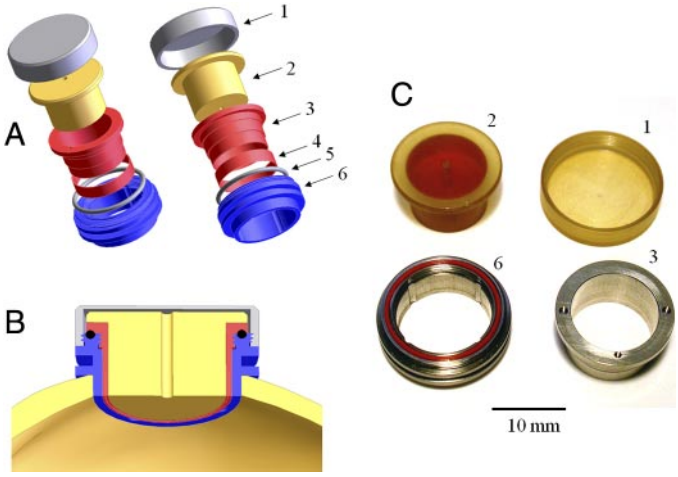

FIG. 1. Design and assembly of the recording chamber system. *A*: exploded view of the design drawing of the chamber system in 2 orientations. *B*: cutaway view of the fully assembled chamber system mounted onto a 3-dimensional (3D) cranial model of a monkey's skull. The colors of the chamber system components are the same as depicted in *A*. *C*: fabricated components of the chamber system. Numbers in *A* and *C* indicate the following components: 1, cap; 2, plug; 3, sleeve; 4, retaining ring; 5, O-ring; 6, chamber.

would lie in direct contact with the surface of the dura. To satisfy both constraints, we chose to use a thin membrane of Sylastic (Dow-Corning, No. 7–4107) that had been successfully employed in optical imaging experiments in non-human primates (Arieli et al. 2002). While allowing easy passage of the electrodes, the membrane's ability to reseal is limited to a relatively small number of electrode penetrations (5–10 at a single site). It therefore became necessary to make the membrane replaceable after its seal becomes compromised. Our second objective was to keep the diameter and height of the chamber small, so that multiple chambers could be implanted in a single animal and so that the dural or cortical surface of the brain could be easily accessed during simple surgical procedures.

To accomplish these objectives, we designed the system to consist of five components. Design drawings of the system are shown in Fig. 1*A* and a completed system is shown in Fig. 1*C*. The components include the chamber, a removable sleeve and retaining ring, a plug, a cap, and an O-ring. The chamber, sleeve, and retaining ring are constructed from Titanium (6AL/4V ELI), and the plug and cap are constructed from Ultem plastic. The O-ring is made of silicone 70 durometer red and is manufactured by Sterling Seals.

To bring the Sylastic membrane in contact with the dural surface, we first designed the chamber to have a lower extension of its wall that would fit snugly within a circular craniotomy (Fig. 1*B*). The depth of the lower wall was set to 2 mm so that when implanted its bottom surface would rest gently on the surface of the dura. Depending on the location of the implant, this often required some thinning of the cranial bone to ensure even thickness around the chamber. The sleeve was designed to thread into the chamber, and its vertical dimension adjusted so that its bottom surface would lie flush with the bottom of the chamber wall. To ensure a tight seal between the chamber and the sleeve, we introduced a groove on the chamber's upper surface for placement of an O-ring, and a flange on the upper surface of the sleeve that would overlap the upper wall of the chamber. When the sleeve is fully threaded into the chamber, its flange exerts downward pressure on the O-ring generating a water-tight seal. To attach the membrane to the bottom surface of the sleeve and thus bring it into contact with the dural surface, the outer diameter of the sleeve was stepped down so that a small retaining ring could be easily placed over the end (Fig. 1*A*). This allows the membrane to be mounted by laying it across the bottom surface of the sleeve and then press fitting the retaining ring in place (Fig. 2). When done in this way, the membrane is stretched across the bottom of the sleeve like a drum head. The residual Sylastic can then be removed with a scalpel. Finally, when not in use, the lumen of the chamber is filled with the plug and covered with the protective cap. This provides an abutting surface, similar to the cranium, so that changes in intracranial pressure don't lead to protrusion of the brain through the craniotomy. In early versions of the design, we noticed that the insertion of the sleeve often trapped a bubble underneath the membrane, and in one case, this was sufficient to compress the cortical circulation and produce a permanent lesion. To avoid this problem, we introduced a set of four vertical grooves on the inside wall of the chamber, and a central hole in the plug, to allow air to escape when either the sleeve or the plug are mounted within the chamber.

To provide consistent positioning of the manipulator within the chamber and make the sleeve easy to remove, the upper surface of the sleeve was designed with three small, closed-end holes (Fig. 1*C*). The smaller of the three holes provides for placement of a centering pin on the manipulator, and the remaining two symmetrically placed holes allow for the insertion of a tightening tool. The tool proved to be necessary to obtain a tight seal with the O-ring and to enable the removal of a tightly placed sleeve. Finally, the chamber was designed with an external groove on its outer wall so that acrylic cement could be used to fix the chamber to the skull in combination with Titanium orthopedic bone screws (Synthes). In future versions of the chamber, we plan to incorporate a perforated flange on the bottom of the outer wall that will enable the chamber to be mounted directly with bone screws and eliminate the need for acrylic cement.

Mechanical components of the manipulator system

ASSEMBLED SYSTEM. The micromanipulator was designed to couple to the recording chamber, and provide remote control of eight independently movable microelectrodes. The mechanical components consist of a set of eight linear actuators mounted in a machined aluminum block that is fixed to a frame assembly. Design drawings of the system are shown in Fig. 3, and a completed system is shown in Fig. 4. When assembled, the manipulator consists of seven mechanical and structural components and two printed circuit boards (PCB, see following text). The actuator block houses a set of eight linear

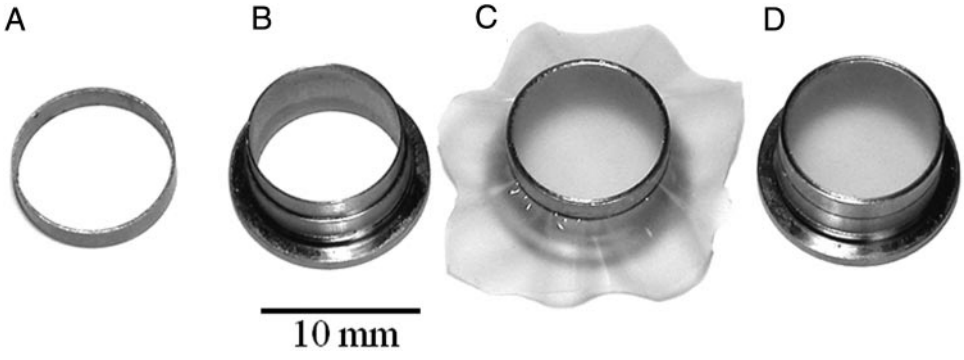

FIG. 2. Mounting of the Sylastic membrane onto the sleeve. *A*: retaining ring. *B*: chamber sleeve. *C*: sleeve and ring after initial placement of the membrane. *D*: sleeve and ring after the membrane has been trimmed.

actuators, the base cone holds the guide cylinder (described in the following text), and the block and base are held together by four support arms. A pair of standoffs allow the motor control PCB to be positioned above the actuator motors, a plastic cap covers the top of the assembly, and two side covers enclose the interior. All of the metal components are made of Aluminum, were machined on a CNC milling machine, and anodized to provide a protective surface.

When fully assembled (Fig. 4*A*), the system is 5.63-in (143 mm) in height and weighs 129.5 g. The outer diameter of the chamber and the protective cap are 0.775 in (19.7 mm) and 1.425 in (36.2 mm), respectively. The inner diameter of the chamber sleeve is 0.5 in (12.25 mm).

LINEAR ACTUATOR. A photograph of a completed linear actuator is shown in Fig. 5. The device consists of a miniature stepping motor (5 mm OD) fitted with a four-conductor flex-print cable, a 1:125 gearbox, a lead screw (100 threads/in), a plunger, and an electrode holder. The motor, gearbox, cable, and lead screw were purchased from MicroMo (No. BL2S5.125.L.0). The plunger is constructed from Ultem-1000 plastic and has two grooves machined along opposite sides of its long axis (Fig. 5, *inset*), a set of internal threads matching those on the lead screw, and a circular hole on the opposite end for mounting the electrode holder. One of the grooves is flat and provides for the placement of a thin Beryllium-Copper (BeCu) strip (0.772-in L, 0.06-in W, 0.002-in thick; Italix) using cyanoacrylate cement. The strip extends over the full length of the plunger and provides for electrical contact between the electrode holder and the signal PCB when the system is fully assembled. The other groove in the plunger is semi-circular and meshes with a cylindrical, stainless steel key pin that fits into the actuator block. When assembled, this mechanism ensures that the rotation of the lead screw is converted to a linear translation of the plunger during activation of the stepping motor. The electrode holder is made of Brass and is mounted on the end of the plunger using a press fit. When mounted, the upper surface of the electrode holder comes into firm contact with the bent end of the BeCu strip. The electrode holder has a beveled hole in its bottom surface for back loading the electrode, and a pair of threaded holes to

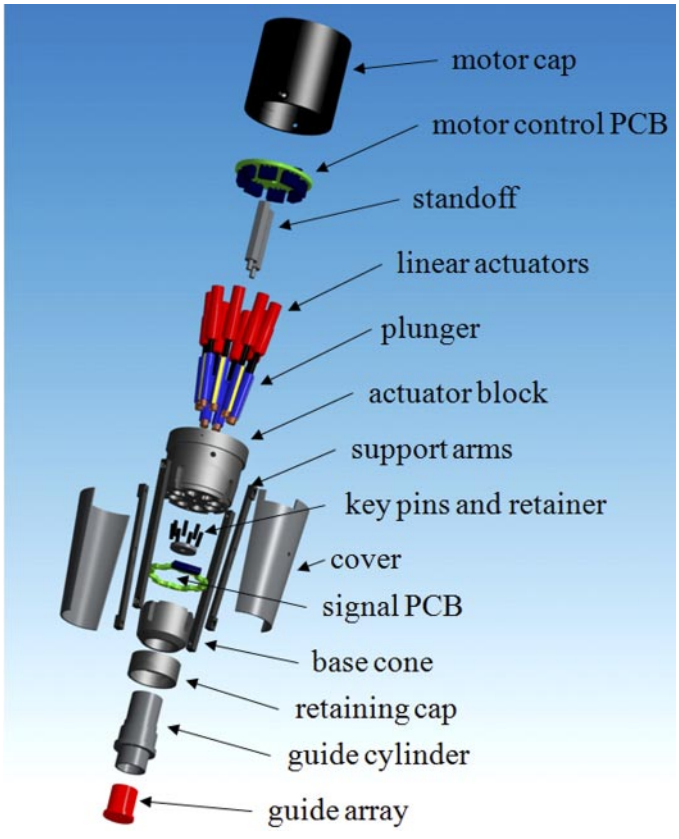

FIG. 3. Exploded view of the design drawings of the microdrive system revealing all component parts and their relative positions within the device.

FIG. 4. Photographs of the fully assembled microdrive (*A*) and a 2nd system with the covers and chamber system removed (*B*). Note the intermediate guide mounted onto the interior of the support arms in *B*.

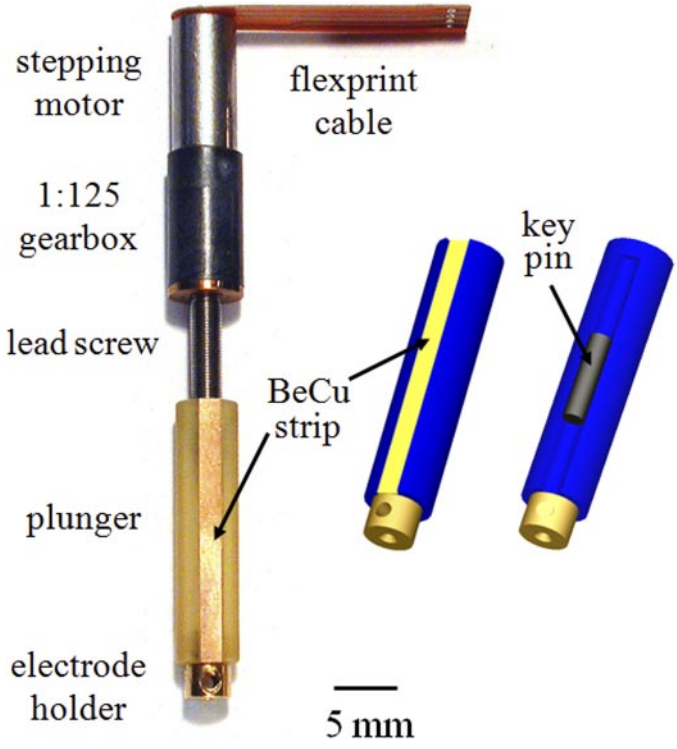

FIG. 5. Photograph of a fully assembled linear actuator. The colored pictures to the right show design drawings of the plunger, illustrating the 2 types of slots machined into the body of the plunger.

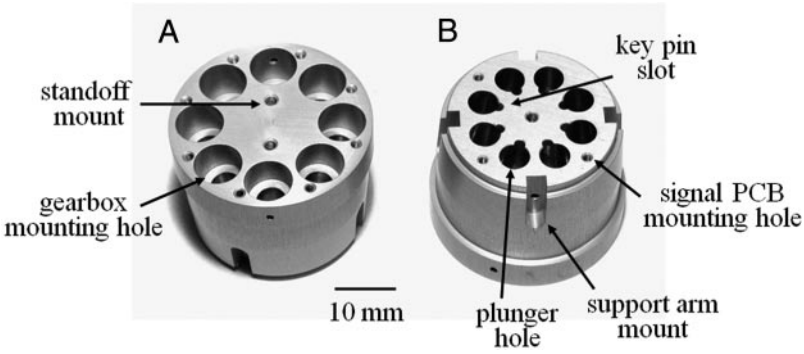

FIG. 6. Photographs of a completed actuator block as viewed from the top (*A*) and bottom (*B*).

mount opposing set screws (1/16 in, 0–80) that enable the electrode to be held firmly in place. The bottom surface of both set screws are ground flat to minimize shearing forces to the end of the electrode.

ACTUATOR BLOCK. A completed actuator block is shown in Fig. 6. The device is machined from a block of aluminum and anodized to protect its surface from scratching and provide electrical insulation. It contains a set of eight holes, drilled at an inward angle of 7°, arranged in a circle for mounting each of the linear actuators. Each hole has two inner diameters, one for mounting of the actuator gearbox (Fig. 6*A*) and a second that allows for smooth passage of the plunger (Fig. 6*B*). An additional slot is milled into the inner edge of the bottom portion of each mounting hole to allow for placement of the key pins. Two threaded holes on the top of the block allow for mounting of standoffs to hold the motor control PCB, and three threaded holes on the bottom of the block allow for mounting of the signal PCB. Four slots, with threaded holes, allow for mounting of the support arms to the bottom portion of the block, and a central threaded hole on the bottom surface allows a circular disc to be mounted for retaining the key pins within the block.

BASECONE, GUIDE CYLINDER AND RETAINING CAP. The lower portion of the assembly consists of two components, the basecone and the guide cylinder (Figs. 3 and 7). The basecone provides the structural framework for linking the actuator block to the guide cylinder. Its upper portion contains slots for mounting the support arms, and its lower portion contains a threaded receptacle for mounting the guide cylinder (Fig. 7*A*). The guide cylinder has several key features that facilitate the alignment of electrodes and the mounting of the microdrive to the recording chamber (Fig. 7*B*). First, it is designed so that a guide array can be press fit into its bottom opening. The tight fit ensures that it will not move or rotate within the cylinder. The guide array is a cylindrical block of Ultem-1000 plastic (0.5-in height) containing an 8 × 8 array of parallel guide holes [0.015 in (0.37 mm) ID, 0.035 in (0.86 mm) spacing] that have been drilled through its long axis. These holes serve as guide tubes for positioning electrodes within the chamber. The bottom end of the guide array is flanged so that it always aligns to the same vertical position when mounted in the cylinder. Second, the guide cylinder is constructed with a flange located approximately one-third of the distance from its bottom surface, and a guide pin is press fit into the lower surface of the flange. When the system is mounted onto a recording chamber, the flange ensures that the bottom surface of the guide array will come to rest at a position slightly beyond the plane of the Sylastic membrane. This ensures a tight apposition between the guide array and the membrane. The guide pin ensures that the guide array will always be mounted at the same position within the recording chamber. Finally, the flange on the guide cylinder also enables the incorporation of a retaining cap, which attaches the microdrive to the recording chamber (Figs. 3 and 4). This cap is mounted onto the guide cylinder before it is threaded into the basecone, and its inner surface contains threads that match those on the outer surface of the recording chamber. When the cap is threaded onto the chamber, it exerts downward pressure on the guide cylinder flange and ensures a tight, vibration free fit between the microdrive and the chamber.

PRINTED CIRCUIT BOARDS. The manipulator is designed to house two PCBs. One board provides connections to the motor control circuitry (see following text) and another to the amplifier headstage. Both boards were manufactured by Trilogy-Net, and are shown in Fig. 8. The motor control PCB (*A* and *B*) is a simple two-layered board that provides connections between each of eight four-pin connectors (Molex, No. 52808×0490) on the bottom surface (*B*) to a single 32-pin, zero-insertion-force, connector (Molex, No. 52559×3292) on the top surface (*A*). Connections are made to the latter connector from the motor control system via a 32-conductor flex-print ribbon cable (Parlex, No. 050×32×1524B).

The second board, shown in Fig. 8, *C* and *D*, is designed to make contact to each of eight electrodes via a spring-loaded sliding contact mechanism. To accomplish this, the board was built in a circular configuration with solder pads arranged in register with the plungers

FIG. 7. Photographs of a completed basecone (*A*) and guide cylinder (*B*). The guide cylinder is shown with (*right*) and without (*middle*) a mounted guide array (*left*).

of each actuator. Electrical contact is established by soldering a short beryllium-copper (BeCu) tab (0.120 × 0.040 × 0.002 in) to each pad so that it extends 2 mm toward the center of the circuit board (Fig. 8, *C* and *D*). This ensures that when the PCB is mounted onto the actuator block, each BeCu tab is gently pressing against the corresponding BeCu strip of the plunger thereby making a spring-loaded contact.

The BeCu tabs and strips were made by Italix (Santa Clara, CA). They were cut, bent, heat treated, and cleaned. The tabs were soldered onto the PCB during the final step in manufacture of the boards (Trilogy-Net). The connector making contact with the amplifier headstage consisted of nine pins having a pitch of 0.05 in. This connector was compatible with MultiChannel Systems headstage (MPA8I); however, the connector can be easily replaced to accommodate other types of headstage amplifiers.

Assembly

For assembly, the lead screw on each actuator is fitted with a plunger and electrode holder (Fig. 5) and then mounted into one of the holes in the actuator block (Fig. 6*A*). The flexiprint cable attached to each motor is folded upward and inserted into the corresponding connector on the underside of the motor control PCB (Fig. 8*B*). The PCB is then fixed to the standoffs that are mounted on the top surface of the actuator block. The key pins are then placed into each hemispherical slot on the underside of the actuator block, and the retaining plate is screwed in place. Once this step is completed, the signal PCB is gently placed over the ends of the plungers and fixed in place with cap screws. During this step, it is important to insure that the BeCu tabs do not catch on the ends of the plungers or electrode holders, otherwise they will be bent backwards and will have to be repaired or the PCB replaced. Figure 9 shows a bottom-up view of an assembled microdrive before the support arms and basecone are attached. *B* shows a magnified view of the sliding contact between the BeCu tabs on the signal PCB and the BeCu strips mounted on each plunger. *C* shows the relationship between the key pins mounted within the actuator block and the semicircular groove in each plunger. In the final steps of the assembly, the support arms are mounted onto the basecone and the actuator block. The retaining cap is placed over the guide cylinder, which is then threaded into the basecone (see Figs. 3 and 4 for details).

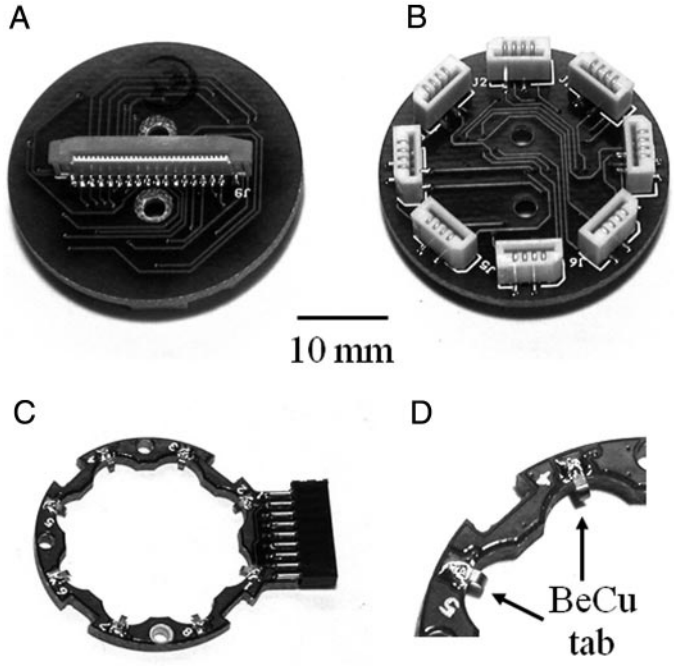

FIG. 8. Photographs of the motor control printed circuit boards (PCB; *A,* top view; *B,* bottom view) and the signal PCB [*C,* top view; D, magnified to illustrate the beryllium-copper (BeCu) tabs].

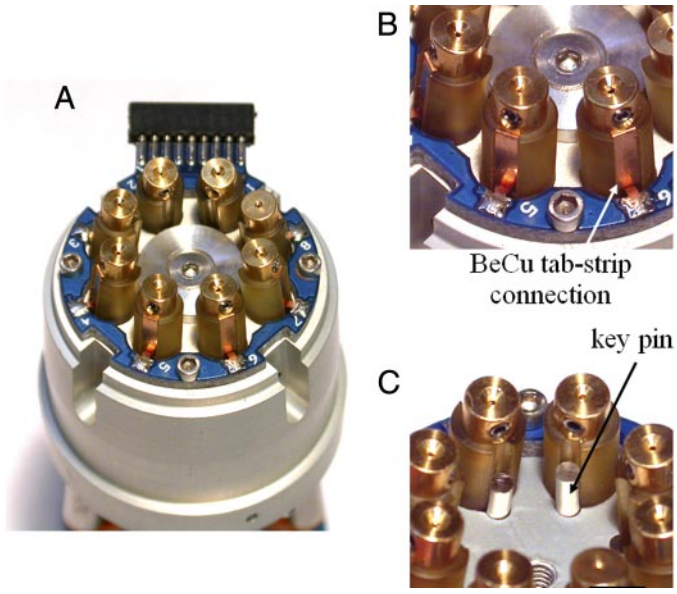

FIG. 9. Photographs of the underside of an assembled actuator block with the linear actuators and signal PCB mounted. The support arms and covers have been removed to permit a clear view. The picture in *A* shows the fully assembled device. *B* shows a magnified view to illustrate the connection between the BeCu strips and tabs. *C* shows the how the key pins fit within the actuator block to stabilize the position of the plungers. The retaining washer has been removed for visualization.

Motor control system

The control system that interfaces to the micromanipulator consists of two main parts, a rack-mounted electronic motor controller (EMC), and a remote motor interface unit (RMIU). A schematic diagram of the control system architecture is shown in Fig. 10, and photographs of the printed circuit boards are shown in Fig. 1 of the supplementary materials.[1] The main component in the EMC is the Atmel ATmega128 8-bit RISC microcontroller operating at 14.7456 MHz. This device communicates with a monitoring and control computer via a serial connection, stores the positions of all the motors, and provides the control signals for the timing of the stepping motors. Software for the microcontroller was written in C, converted to assembly code and downloaded using the software package AVR Studio 4 (Atmel). The serial connection transmission rate is set at 115,200 bit/s for fast continuous updates of motor positions. The serial communication protocol utilizes ASCII command strings, which are newline character terminated. Error detection is accomplished using an odd-parity bit. The high level serial (RS-232) signals are level shifted to the I/O voltages required by the microcontroller using a MAX232 interface chip.

The RMIU controls motor selection and delivers current to the selected motor. Each unit houses eight removable motor control cards, each capable of driving eight stepping motors. The cards are mounted in a backplane card, capable of mounting eight control cards to provide control of ≤64 motors (Fig. 1, *B* and *D,* supplementary material). Each control card has its own shift register (SN74HC595D, Texas Instruments), to enable motor selection, and a single N-channel (IRF7456) and three P-channel MOSFETs (IRF7210, International Rectifier) to provide current to each motor. The shift register of each control card is connected serially to that of the adjacent cards via the

[1]The online version of this article contains supplemental data.

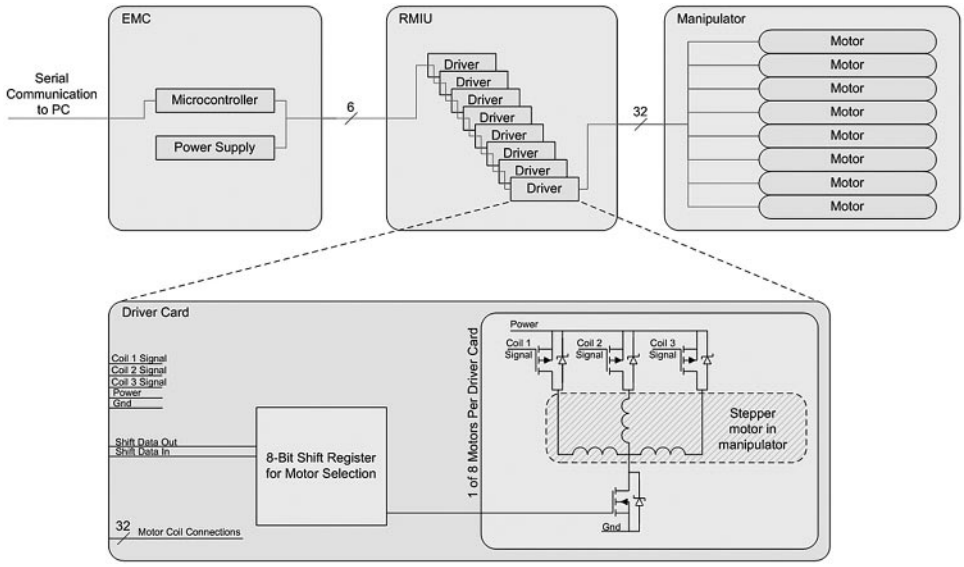

FIG. 10. Architecture of the motor control system. A schematic of the electronic motor controller (EMC), a remote motor interface unit (RMIU), and manipulator are shown at top. Details of a single motor driver card are shown below. Software on the PC relays commands to the microcontroller on the EMC over the serial connection. The microcontroller selects a motor by shifting a single selection bit into the shift register on the driver card. Each driver card can drive 8 motors and has a shift register which can be daisy chained to another card for motor selection across multiple driver cards. The microcontroller then activates the motor coil transistors to drive the stepper motor in the manipulator.

backplane card. This allows the microcontroller to select a specific motor on any of the eight control cards.

Communication between the EMC and the RMIU is routed through an eight conductor cable carrying power, coil signals, and motor selection data. To select a specific motor, the microcontroller shifts a data word, containing a single high bit, into the shift registers on the motor control cards in the RMIU. When the shift register output is latched, the selected N-channel MOSFET connects the common coil wire to ground on the stepping motor. All other motors are kept inactive because their connection to ground is held at high-impedance. The microcontroller then switches the P-channel MOSFETs to connect the motor coils to +5 V in sequence to move the motor (see Fig. 10).

Each manipulator is connected to the RMIU by a 32-conductor flat flex cable (Parlex). The connectors for these cables (52559×3292, Molex) are mounted on the back side of the RMIU card (Fig. 1*D,* supplementary material).

Software

The graphical user interface (GUI) was written in the C language using the National Instruments GUI libraries for user control, runs on the Windows operating system, and communicates with the EMC by serial/RS-232 protocol. Figure 2 in the supplementary material shows a screen shot of the GUI that provides user input to control the micromanipulator. The user can set the motor speed, control the direction and the number of steps for each movement command, and set the movement resolution of the device according to the number of threads/inch on the lead screws. Once a motor is selected, the position reading can be zeroed, and each electrode advanced independently. At the end of a session, all of the electrodes can be returned to their zeroed positions using a GUI command.

Microdrive parameters

The operating parameters of the microdrive system are given in Table 1 and are based on measurements taken from seven fully assembled systems.

RESULTS

Chamber system and dural removal

During the past 3 years, we have implanted chambers, and performed subsequent electrophysiological recordings, at 11 locations in five monkeys. At all but three locations, the chambers were positioned over area V1 near the occipital pole. In one animal, a chamber was implanted over area V4, and in another animal, we implanted two chambers at the same time, one over the intraparietal sulcus, and a second over the principal sulcus. Although it is not necessary to remove or thin the dura to use this chamber system, we tested the performance of the chamber under such conditions. At five of the chamber sites, we completely removed the dural membrane overlying the cortex. This was done after the chamber was implanted by carefully lifting the dura using a pair of fine forceps and incising the membrane around the inner perimeter of the chamber using a No. 11 scalpel. At the remaining six locations, we thinned the dura prior to recording by carefully peeling away several layers of the membrane until the underlying cortical vasculature was just visible. In all instances, we performed these procedures using sterile technique, and the tissue was flushed using artificial cerebrospinal fluid (ACSF) at physiological pH (7.2–7.4) and temperature (38°C) (Arieli et al. 2002). The use of ACSF greatly reduced the amount of bleeding compared with similar procedures done with physiological saline. To further reduce the inflammatory response of the dura, the animals were given dexamethazone (im) during and after the surgery at 24-h intervals for 5 days (0.5 mg/kg).

We typically began neuronal recording 2–3 days after removing or thinning the dura. At those sites where the dural membrane was removed, we observed two types of tissue responses that were visible through the Sylastic membrane using an operating microscope. In two cases, the cortical surface was in direct contact with the Sylastic membrane, presumably due to positive intracranial pressure. This was the response we had hoped for when designing the chamber system, and it allowed accurate recordings of neuronal activity

TABLE 1. *Properties of electrode movement*

Electrode Travel, mm	Travel Resolution, μm/step	Maximum Velocity, μm/s	Positional Lag, μm
11	0.66 μm/step	168	70–100

to be made from the upper layers of the cortex. In the other three cases, the cortex appeared to lie 1–2 mm below the Sylastic membrane, with clear CSF filling the space. In all five cases, we observed a gradual invasion of granular tissue over the surface of the cortex that eventually led to the replacement of the dural membrane. This process varied in rate from one chamber site to another, and typically was complete by 6–8 wk after the initial dural removal. In two cases, we attempted to prevent the growth of this membrane by first removing the sleeve and then removing the connective tissue with forceps. This approach was largely ineffective because regrowth was rapid and in one instance we damaged some of the small pial vessels.

Overall, our approach to the problem of dural regrowth differed substantially from that of Arieli et al. (2002). In their study, it was essential that the dural membrane be prevented from re-growing, otherwise optical imaging from the cortical surface would become impossible. Our objective in removing the dura was to facilitate the entry of multiple electrodes into the surface cortex and avoid the substantial dimpling that occurs in these procedures when the dura is intact. We therefore made no attempt to block the re-growth of the dura and did not carefully track the time course or properties of the dural regrowth.

Once the regrowth of the dural membrane was complete, we made several attempts to remove the newly formed dura. In general, we found this to be difficult, as it appeared to us that the dura had become integrated with the pial surface during its regeneration. Attempts to remove it led to slight damage of the pial vessels in two instances. Overall, we found that the best approach was to leave the original sleeve in place and avoid any manipulations of the tissue for as long as possible. When we took this approach, we could routinely make electrode penetrations into the surface cortex without any detectable dimpling for periods lasting 4–6 wk. Once the regrown dura had thickened, thinning procedures could be done with little or no difficulty.

At the six chamber sites where the dura was thinned, but not completely removed, electrodes would readily penetrate the dura for a period of 2–4 wk. After this period, it became necessary to repeat the dural thinning procedure. We repeated this procedure as many as six times allowing for 3–6 mo of reliable recording. At these sites, the interior of the recording chamber remained free of infection.

Electrophysiological recording

We have performed extensive multielectrode recordings of neuronal activity using three of the microdrive systems. In general, the system has performed well (problems are discussed in the following text) and high quality broadband (1 Hz to 10 kHz) recordings, having low noise, were readily obtained on a daily basis. An example of raw data collected on one such recording is shown in Fig. 11. In this experiment, four electrodes were advanced into area 7a of the posterior parietal cortex. A broadband signal was sampled from each electrode, enabling subsequent separation of the local field potential signal (1–150 Hz) and a high-pass signal containing unit activity (500 Hz to 10 kHz). Single-unit activity was extracted off-line from the high-pass signal using a semi-automated spike sorting algorithm (Goodell and Gray 2003; Yen et al. 2006).

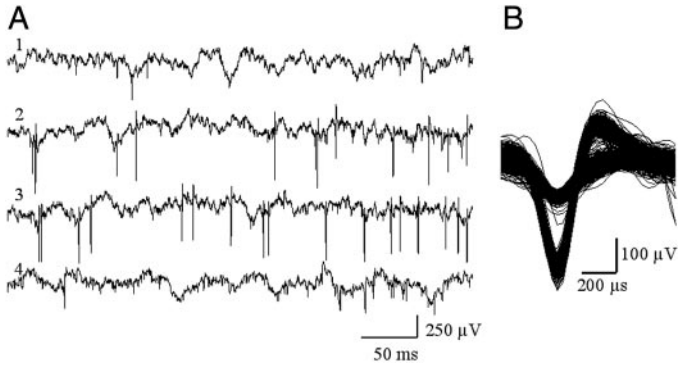

FIG. 11. Example data collected from 4 electrodes during a single recording session. *A*: short epoch of raw data sampled from 4 electrodes in area 7a of the posterior parietal cortex of an alert monkey. The signals are broadband (1 Hz to 10 kHz). Extracellular action potentials are visible as negative going spikes in the signals. *B*: plot of 1,000 superimposed waveforms extracted from the high-pass filtered signal on channel 3. The high-amplitude waveforms reveal a single unit that is well separated from the lower amplitude multiunit activity.

On a typical recording session, prior to mounting the manipulator on the animal, and after sterilization of the electrode tips, we positioned each electrode so that its tip was just visible at the distal opening of the guide hole. The electrode position was set to zero using the GUI. Each electrode was then retracted 0.5 mm to avoid damage to the tip during mounting. The microdrive was mounted on the chamber and the electrodes were advanced sequentially in increments of 100 steps (67 μm). When an electrode passed through the Sylastic membrane, a clear transition from open-circuit noise to a detectable field potential could be observed. This typically required 100–300 μm of movement from the zero position. We usually advanced all of the electrodes to this point, when recording from surface cortex, before beginning the search for neuronal activity. This helped to minimize subsequent mechanical disturbances because the dimpling of the membrane occurred before any neuronal activity was isolated. The electrodes were then sequentially advanced in 100-step increments until multiunit activity could be detected on at least one electrode. At this point, electrode movement was reduced to 10- or 20-step increments. Subsequent movements were then used to maximize the signal-to-noise ratio of the unit activity.

Several aspects of this recording sequence are noteworthy. First, well-isolated single units were not always recorded simultaneously on every electrode. This is evident in Fig. 11. Attempts to improve the isolation on one electrode often influenced the isolation of units on adjacent electrodes. Because of this, we found that the best way to maximize unit isolation across electrodes was to first obtain multiunit activity on all the electrodes, let the recording stabilize for 10–30 min (or longer) and then make small gradual changes in electrode position (1–10 μm) to improve signal quality. When well-isolated units were obtained, it was often helpful the retract the electrode to improve or maintain the isolation. Second, because of the large currents needed to activate the stepping motors, it was not possible to monitor neuronal activity during electrode movement. This usually was not a problem because small movements were completed in less than a second. Third, because the microdrive was designed to act as its own Faraday

cage, interference from 60-Hz line noise was often undetectable. This enabled recording of the broadband signal without the need for additional shielding or filtering. Finally, recording stability was typically very good. Isolated units could routinely be held for periods lasting 1–2 h. The principal factor affecting recording stability was the presence of an air-tight seal within the chamber. Recording stability was compromised whenever an air bubble was present below the surface of the Sylastic membrane prior to recording. This often led to detectable cardiac pulsations in the broadband signal and consequent variations in signal quality.

Sylastic membrane

The Sylastic membrane appeared to have very little effect on the recording properties of our electrodes. After repeated recordings using a variety of electrode parameters, we settled on the use of Tungsten-in-glass electrodes manufactured by Alpha Omega (125 μm wire, 300 μm OD, 1 MΩ impedance, 60° taper angle). Electrodes of smaller diameters, or finer tip tapers, occasionally had bent tips or reduced impedance after penetrating the Sylastic membrane. With the current electrode parameters, we routinely used the same electrodes three to six times and usually found little or no change in the electrode impedance, when tested at 1 kHz. We and others have also successfully used other types of electrodes, including epoxy coated Tungsten electrodes manufactured by FHC (M. Leslie, Vanderbilt University, personal communication).

The Sylastic membrane also showed little resistance to electrode penetration and, in most cases, was self-sealing. Evidence for this was apparent in those instances where the dural membrane had been completely removed. In some of these recordings, we encountered neuronal activity within 400 μm of the starting position of the electrode within the guide tube. This indicates that very little dimpling of the membrane occurred.

There was often a small droplet of residual fluid present on the surface of the membrane once the electrodes had been withdrawn. This suggested that the membrane had either not completely sealed around the electrode during a recording or had not resealed after the electrode was withdrawn. The amount of residual fluid was always very small, and we found no evidence that fluid from the cranial cavity had wicked up into the holes in the guide array. This suggests that the residual fluid had escaped during withdrawal of the electrodes. In these cases, we usually removed the fluid with gentle suction, using a sterile pipette, before sealing the chamber and returning the animal to its cage. This manipulation appeared to facilitate the resealing of the membrane as we often found the chamber to be completely dry the following day. This effect was not repeatable indefinitely, however. The membrane typically began to leak after 5–10 electrode penetrations at the same site. When this occurred small amounts of fluid would accumulate in the chamber.

When electrophysiological recordings were not being performed, the Sylastic membrane maintained a stable water-tight seal for many months. In one animal, the membrane was left in place for 18 mo before the dura was thinned, and recordings were begun. At the time of thinning, the dural membrane was healthy and appeared only marginally thicker than it was at the time the craniotomy was performed.

In general, infections have been either rare or nonexistent. This has been one of the big benefits of the technique because maintaining a sterile barrier eliminates the need for daily cleaning of the chamber and reduces the rate of regrowth of the dural membrane. When infections have occurred, they have been very difficult to eliminate as is often the case with conventional recording chambers. In these instances, we have found it necessary to remove the sleeve and replace it with a sterile sleeve two to three times each week. This procedure can be done in 10–15 min, without anesthetizing the monkey, provided aseptic technique is used.

Using multiple microdrives

One important advantage of the system is that it permits the simultaneous use of multiple microdrives, enabling the sampling of neural activity from multiple brain areas. This is possible because of the small dimensions of the chamber, the relatively small size and light weight of the microdrive, and the capability of the electronics and software to operate $\leq$64 motors at a time. We made use of this capability in one monkey by implanting two recording chambers, one over the intraparietal sulcus, targeting areas 7a and LIP, and one over the principal sulcus, targeting areas 9 and 46 of the prefrontal cortex. In general, the addition of a second chamber posed no significant mechanical obstacles other than increasing the time needed to prepare the microdrives and advance the electrodes during each recording session. Electrically, however, the addition of a second microdrive presented at least two difficulties. First, because the microdrive is designed so that the ground connection passes through the recording chamber, the addition of a second chamber introduced the possibility of creating a ground-loop, and hence significant line noise. Second, because each drive is fitted with an 8-channel connector, it became necessary to use either two 8-channel amplifiers or to build an adapter that would connect all 16 channels to a single 16-channel headstage. We solved the ground loop problem by using only a single ground and passing all of the signals to a single main stage amplifier.

DISCUSSION

We have designed, built, and extensively tested a new type of chamber and microdrive system for performing acute multielectrode recordings of neuronal activity in awake behaving monkeys. The system offers a number of advantages over existing technology. The chamber is small, is low in profile and incorporates a replaceable sleeve containing a thin Sylastic membrane that is easily penetrated by microelectrodes. The small size minimizes the amount of cranial surface area taken up by the chamber and facilitates the implantation of multiple chambers on a single animal. The low profile permits easy surgical access to the chamber interior, which facilitates procedures such as dural thinning or removal. The replaceable sleeve allows a hermetic seal to be established. This greatly reduces the susceptibility to infection, eliminates the need for daily cleaning, and reduces the rate of dural thickening that occurs in the absence of a seal. The seal also permits complete removal of the dural membrane, a manipulation that would otherwise be very risky with conventional chambers. The Sylastic membrane is very thin, can be easily penetrated with

multiple microelectrodes without changing their recording characteristics, and, when coupled with thinning or removal of the dura, greatly reduces dimpling of the tissue thereby permitting more accurate tracking of electrode depth in the cortical tissue.

The microdrive and electronic control system also offer several advantages over existing technologies. The device is easy to use and relatively small in size and weight, couples directly to the chamber system, requires no special accessory devices to operate, and acts as its own grounded Faraday cage to eliminate line noise and permit broadband recording. The control system is operated by a personal computer, via serial port communication, running the Windows operating system, and can control ≤64 motors with no design change. Together this design increases the versatility for performing multielectrode recordings in alert monkeys. We expect that future refinements in the existing design will further increase their flexibility and reliability for a wide variety of uses.

Technical problems and future modifications

As with any new technology, a number of minor technical problems were encountered, and the need for additional design changes became apparent, both of which deserve comment. With respect to the chamber system, the current design requires that acrylic cement be used to fix the device to the animal's skull. This has worked well, but the design would be improved by directly fixing the device to the skull. This would serve to reduce the overall dimensions of the implant and potentially reduce the susceptibility to infection. A simple way to implement this capability would be to design the chamber with legs or a mesh radiating parallel to the cranial surface that could be fixed directly to the skull with orthopedic bone screws. This would increase the fabrication cost of the chamber but could be easily implemented with conventional machining techniques. Another limitation of the chamber is that it is designed to be implanted tangential to the cortical surface. This limits the number of locations that can be targeted because the increase of soft tissue at more lateral locations interferes with the use of the chamber. This problem can be solved by redesigning the chamber to mount vertically, but optimizing the design requires prior knowledge of the dimensions of the skull at the target site so that the lower surface of the chamber can be machined to fit each animal's skull at a particular recording location. Although this can be accomplished by reconstructing the cranial surface from a CT scan (Gray and Goodell 2005), it will substantially increase the cost for each chamber. Moreover, the internal sleeve would have to be redesigned to mount vertically within the chamber, and it would not be possible to incorporate the Sylastic membrane in the current manner. Finally, it would be useful to construct the chamber out of plastic to make it compatible with magnetic resonance imaging. We see no fundamental problems with this other than the possible need to increase the thickness of the retaining ring for mounting the Sylastic membrane onto the sleeve.

With respect to the microdrive and control system, a number of useful design changes became apparent after extensive use of the system. These included mechanical, electrical, and software changes. Mechanically, we discovered three problems that limited the performance of the system. First, the actuators consistently displayed ~70–100 μm of positional lag when reversing movement direction, making accurate electrode positioning difficult whenever a change of direction was required. We were unable to effectively reduce the lag by improving the precision of the threads on the plunger without also increasing the friction on the lead screw. The best solution is to compensate for the lag in the control software by incorporating a position offset equal to the magnitude of the lag. A second mechanical problem became apparent over time as the dural membrane increased in thickness. At the beginning of recording sessions, when the electrodes were being advanced through the dura, the electrode shafts would occasionally bend rather than penetrate the dura. This was due to the small wire diameter of our electrodes (100 μm, 300 μm with glass insulation) and the long span between the electrode holder and the top of the guide array. We solved this problem by incorporating a set of eight stainless steel guide tubes that could be press-fit into selected holes in the top of the guide array prior to recording, and held in alignment with each actuator using a grid mounted on the interior of the support arms (the grid is visible in the middle of the microdrive in Fig. 4*A*). Finally, we also found that it was easy to mistakenly retract or advance the actuators beyond their upper and lower positional limits. When this happened, there were times when the resulting friction would cause the plunger to stick in place, and these instances were not registered by the software and were thus not detected by the user. Short of incorporating a separate position encoder for each actuator, which we ruled out due to size, complexity and expense, the best solution is to incorporate end limits within the software which can be set at the beginning of each recording session.

Electrically, we found very few problems overall. The only consistent difficulty, which showed up after prolonged use of the system, was the presence of occasional intermittent signal connections between the BeCu tabs on the PCB and the BeCu strips on the plungers. We discovered that these problems were due either to the build up of an oxidation layer on the surface of the BeCu contacts or a slight bending of the tabs making the connection between strips and tabs unreliable. We solved the first problem by occasionally cleaning the surfaces of the contacts. The latter problem was solved by redesigning the BeCu tabs so that they were thicker and longer. This increased the force of the spring loaded contact between the tabs and the strips on the plungers.

Although we have mentioned several changes to the software that improved the design or eliminated problems, we also found that the system could be greatly improved by including software modifications to permit automated electrode movement sequences. This was particularly evident when advancing multiple electrodes each day, which often required a great deal of time by the user. This capability should be relatively easy to implement and would enable the user to specify a wide variety of movement sequences.

ACKNOWLEDGMENTS

We thank M. Leslie at Vanderbilt University for valuable comments on an earlier version of the manuscript. We also thank R. Himmelspach for excellent care of the animals.

GRANTS

This material is based upon work supported by National Science Foundation Grant 0138848. This work also was supported by a grant to C. M. Gray

from the program for Instrument Development for Biological Research at the National Science Foundation.

REFERENCES

Asaad WF, Rainer G, Miller EK. Task-specific neural activity in the primate prefrontal cortex. *J Neurophysiol* 84: 451–459, 2000.

Arieli A, Grinvald A, Slovin H. Dural substitute for long-term imaging of cortical activity in behaving monkeys and its clinical implications. *J Neurosci Methods* 114: 119–133, 2002.

Baker SN, Philbin N, Spinks R, Pinches EM, Wolpert DM, MacManus DG, Pauluis Q, Lemon RN. Multiple single unit recording in the cortex of monkeys using independently moveable microelectrodes. *J Neurosci Methods* 94: 5–17, 1999.

Cham JG, Branchaud EA, Nenadic Z, Greger B, Andersen RA, Burdick JW. Semi-chronic motorized microdrive and control algorithm for autonomously isolating and maintaining optimal extracellular action potentials. *J Neurophysiol* 93: 570–579, 2005.

Goodell AB, Gray CM. Semi-automated solution to the spike overlap problem using tetrode data obtained from cat visual cortex. *Soc Neurosci Abstr* 429.9, 2003.

Gray CM, Goodell AB. Targeted semi-chronic recording from multiple sites in multiple visual cortical areas in alert monkeys. *Soc Neurosci Abstr* 569.16, 2005.

Miller EK, Erickson CA, Desimone R. Neural mechanisms of visual working memory in prefrontal cortex of the macaque. *J Neurosci* 16: 5154–5167, 1996.

Mountcastle VB, Reitboeck HJ, Poggio GF, Steinmetz MA. Adaptation of the Reitboeck method of multiple microelectrode recording to the neocortex of the waking monkey. *J Neurosci Methods* 36: 77–84, 1991.

Prut Y, Vaadia E, Bergman H, Haalman I, Slovin H, Abeles M. Spatio-temporal structure of cortical activity: properties and behavioral relevance. *J Neurophysiol* 79: 2857–2874, 1998.

Reitboeck HJ, Werner G. Multi-electrode recording system for the study of spatio-temporal activity patterns of neurons in the central nervous system. *Experientia* 39: 339–341, 1983.

Spinks RL, Baker SN, Jackson A, Khaw PT, Lemon RN. Problem of dural scarring in recording from awake, behaving monkeys: a solution using 5-fluorouracil. *J Neurophysiol* 90: 1324–1332, 2003.

Yen SC, Baker J, Gray CM. Heterogeneity in the responses of adjacent neurons to natural stimuli in cat striate cortex. *J Neurophysiol* 97: 1326–1341, 2007.